Measurements of the $^{33}S(n,\alpha)^{30}Si$ cross-section at n_TOF and ILL: Implications in neutron capture therapy

Javier Praena[1,*], *Isabel* López-Casas[1], *Marta* Sabaté-Gilarte[2,3], *Fernando* Arias de Saavedra[1], and *Ignacio* Porras[1]

[1]Universidad de Granada, Granada, Spain
[2]European Organization for Nuclear Research (CERN)
[3]Universidad de Sevilla, Seville, Spain

Abstract. Up to a couple of years ago, the $^{33}S(n,\alpha)^{30}Si$ cross-section data had been limited and scarce. The origin in the solar system of ^{36}S had been the only motivation to study that cross-section. However, a few years ago, the $^{33}S(n,\alpha)^{30}Si$ reaction was proposed as a possible target in neutron capture therapy (NCT) due to the excellent bio-properties of ^{33}S and the significant resonance at 13.45 keV of the cross-section for which a high-energy α is emitted. Prior to the experiments carried out at n_TOF-CERN and at the Institut Laue-Langevin (ILL) facilities, the data situation was: no data from the thermal point up to 10 keV; from 10 keV to 300 keV, there was only one (n,α) measurement able to resolve the resonances with a questionable value of the 13.45-keV resonance; and the thermal point did not have a consistent value. Here we summarize three experiments that have been performed covering the whole energy range of interest in NCT and astrophysics. These experiments have solved the most important issues. The data of the present work and the evaluated data are used to calculate the dose rate in the tissue.

1 Introduction

The quantity and the quality of nuclear data in a given reaction depend on several issues such as the field of application and the request accuracy. Up to a few years ago, the $^{33}S(n,\alpha)^{30}Si$ cross-section had been only a role in astrophysics due to the origin of the neutron-rich isotope ^{36}S [1, 2], which remains an open question [3]. Few years ago, a possible application of the $^{33}S(n,\alpha)^{30}Si$ reaction to neutron capture therapy (NCT) was proposed by Porras [4].

NCT is a type of experimental radiotherapy whose objective is the selective destruction of tumor cells with high-energy light ions emitted by means of neutron capture in a target element. For this purpose, a binary method is used which combines the absorption of a defined neutron target by tumor cells and the subsequent radiation with neutrons of the tumor area [5].

NCT studies have been focused on ^{10}B as target for neutrons because of several reasons: a very high thermal cross-section of neutron capture with emission of light ions, a high positive Q-value (2.79 MeV) [6] and boron compounds which are absorbed by tumor cells in a greater proportion than in normal cells with a maximum of 3:1 [7]. Therefore, in boron neutron capture therapy (BNCT), a beam of thermal neutrons ($E_n < 0.5$ eV) [8] is captured by boron within tumor cells with the subsequent emission of light ions (α and ^{7}Li) with a high linear energy transfer (LET) in a spatial range within a cell size [5].

IAEA established the figures of merit of a neutron beam suitable for NCT [8]. Briefly, three energetic groups for thermal ($E_n < 0.5$ eV), epithermal (0.5 eV $< E_n <$ 10 keV) and fast ($E_n >$ 10 keV) neutrons were defined and the recommendation for the fluxes (Φ) are the following: $\Phi_{th} \geq 10^9$ n·cm^{-2}·s^{-1} with $\Phi_{th}/\Phi_{tot} \geq 0.9$ for shallow tumors, and $\Phi_{epi} \geq 10^9$ n·cm^{-2}·s^{-1} with $\Phi_{epi}/\Phi_{th} \geq 100$ and $\Phi_{epi}/\Phi_{fast} \geq 20$ for deep tumors.

The ^{33}S interest in NCT is due to: a very large resonance at 13.45 keV, with emission of light ions with a value greater than $^{10}B(n,\alpha)^7Li$ [2]; a very high positive Q-value (3.49 MeV), higher than ^{10}B [6]; and in relation to compounds that transport ^{33}S to tumor cells, a high absorption of ^{35}S in tumor cell has already been observed in mice in *in vivo* experiments [9]. Unlike boron, sulfur is one of the essential elements of living matter and is part of countless compounds that play an important biological role. It is present in the aminoacids cysteine and methionine, in peptides and proteins. Sulfur plays a fundamental role in the synthesis of glutathione, from L-cysteine. The measured concentrations of glutathione in tumor cells are usually high and, in fact, it is considered an important factor in tumor resistance to chemotherapy [10]. The possibility of selectively incorporating a sulfur isotope by glutathione precursors is very promising.

Hence, the status of the $^{33}S(n,\alpha)^{30}Si$ cross-section data, before the role in NCT was proposed, was the following: there was no data from the thermal point up to 10 keV, the most important range for NCT with the present IAEA recommendations; there was only one (n,α) measurement able to resolve resonances [2] which encompassed from 10 keV to 1 MeV, and the thermal point did not have a consistent value due to the few dissenting existing values

*e-mail: jpraena@ugr.es

ranging from 8 to 180 mb [11–14]. In addition, the most important resonance value (13.45 keV), which is essential for the possible use of ^{33}S in NCT, was questioned because of the discrepancies in the resonance parameters between Wagemans *et al.* [2] and the transmission measurement of Coddens *et al.* [15]. Both experiments were carried out in different facilities but the analysis was performed in collaboration. The Γ_α parameter of the 13.45 keV resonance provided by Coddens *et al.* was a factor two that of Wagemans *et al.* [2, 15]. This discrepancy is crucial for NCT because it means that the dose rate could be double in the same treatment conditions (neutron fluence and ^{33}S concentration).

On the other hand, it should be noticed that the most relevant resonance located at 13.45 keV, which is fundamental for the possible use of ^{33}S in NCT, is not in the range of epithermal neutrons (up to 10 keV). However, this limit was established by IAEA with the experience of neutron beams in nuclear reactors and it is expected to be modified with the new generation of accelerator-based neutron sources (ABNS) under development in few projects worldwide [16]. Indeed, it has already been shown that the range where neutrons are considered suitable for human tissue can be increased up to 20 keV [17] or 40 keV [18].

Therefore, new measurements, which would provide the optimal values of the resonance width, were needed for a more realistic estimation of the dose rate in tumor delivered by the $^{33}S(n,\alpha)$ reaction. So, a series of experiments were proposed to INTC committee at CERN with the intention of clarifying all open questions regarding this cross-section [19, 20]. Also, an experiment was proposed to the Institut Laue-Langevin (ILL) committee for the measurement of the thermal point at PF1B line [21]. In the following, the most important results are summarized. Then, the dose rate in ICRU-4 tissue is estimated by means of Monte Carlo simulations with the present data and the ENDF evaluation [22].

2 The experiments at CERN and ILL

The first experiment was carried out at Experimental Area 1 (EAR1) of n_TOF-CERN facility, with the aim of resolving the discrepancies in the resonance parameters of the 13.45 keV resonance between Coddens *et al.* [15] and Wagemans *et al.* [2]. EAR1 is 185 m from the neutron production target, therefore, a high energy resolution can be achieved. The technical features of the facility and the characteristics of the neutron beam are described in detail in [23]. Among the high resolution, other beam characteristic is the large beam aperture, 8 cm diameter, allowing the use of large thin samples that increase the expected low count rate in the resonance valleys. Using borated water as moderator it minimizes neutron capture in hydrogen, and thus the associated in-beam γ-ray background in neutron capture cross-section measurements. The most important consequence for this measurement was a strong reduction of the thermal peak in the neutron flux. Hence, an excellent description of the resonances was achieved but the energy range was restricted from 10 to 300 keV due to the very low count rate below 10 keV. The cross-section was obtained using $^{10}B(n,\alpha)^7Li$ standard. The most remarkable result was that the area of the resonance at 13.45 keV was a factor 1.5 that of Wagemans *et al.*. Regarding the resonance analysis, it was found $\Gamma_\alpha = 100 \pm 5$ eV, in better agreement with Coddens *et al.* (83 ± 3 eV) than with Wagemans *et al.* (41 ± 5 eV). All the details of the experiment and the analysis can be found in [24].

The second experiment was carried out at Experimental Area 2 (EAR2) of n_TOF-CERN facility, with the aim of measuring the cross-section below 10 keV for the first time. EAR2 is located at 20 m from the neutron production target. The increase of the neutron flux, a factor 40 overall, represents the main advantage of EAR2 compared with EAR1. The technical features of EAR2 facility are described in detail in [25]. The cross-section was obtained related to the neutron flux. The most important result was that for the first time the shape of the cross-section was measured from thermal to 10 keV and a $1/v$ behavior was found. The covered energy range was from thermal to 100 keV. The 13.45 keV resonance was resolved with low resolution, however, the area of the resonance was also a factor 1.5 higher than the value of Wagemans *et al.*, confirming the value obtained at EAR1. The final results of the experiment are in progress because of the ongoing extraction of the TOF-energy relation. All the details of the experiment and the analysis can be found in [26].

The third experiment was carried out at PF1B cold neutron line at ILL [27]. The main objective was to obtain the thermal cross-section and to use it as a normalization of the EAR2 data. The cross-section was measured related to the $^{10}B(n,\alpha)^7Li$ standard with different geometries, as well as two ^{33}S samples and two ^{10}B samples. For the first sample and first geometry a preliminary value of 0.25 ± 0.03 barn has been obtained. Figure 1 shows the complete data measured at n_TOF-CERN normalized from thermal to 10 keV with the preliminary data obtained at ILL.

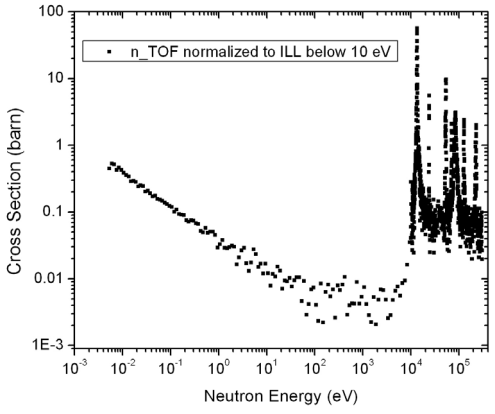

Figure 1. Experimental data obtained at n_TOF-CERN facility. From 10 to 300 keV the data were measured at EAR1. From thermal to 10 keV the data were measured at EAR2. The normalization factor obtained at ILL was applied to the EAR2 data.

3 Dose rate in ICRU-4 tissue with ^{33}S and 13.45 keV neutrons

The calculation of the biological equivalent dose allows the estimation of the success of a treatment. A correct calculation of the biological dose needs a study of the following elements: neutron source, composition and geometry of the tumor, concentration and biodistribution of the tumor dopant, and kerma rates [7, 28]. Kerma rates are an efficient way to study the dose because they provide the absorbed dose which will be supplied by the energy deposited in the tissue [28]. They are calculated according to equation (1):

$$K = \frac{dE_t}{dm} = \phi E \frac{\mu_t}{\rho} \tag{1}$$

where ϕ is the neutron flux and $\frac{\mu_t}{\rho}$, the coefficient that describes the mass energy transferred. Kerma coefficients for neutrons are described based on the number of interactions that occur due to the penetration of neutrons into the tissue, which are defined as (2):

$$k_{fn} = \frac{K}{\phi} = \sum_L N_L \left(\sum_j \sigma_{Lj}(E) \bar{E}_{Lj}(E) \right) \tag{2}$$

being L the sum of all materials; j, the sum of the processes produced; N_L, the density of the material, which is inversely proportional to the atomic mass; and $\bar{E}$, the mean kinetic energy transferred to the charged particles because of the different processes with cross-section σ. Figure 2 shows the kerma coefficients of the reactions on ICRU-4 tissue [29] considered in the present work.

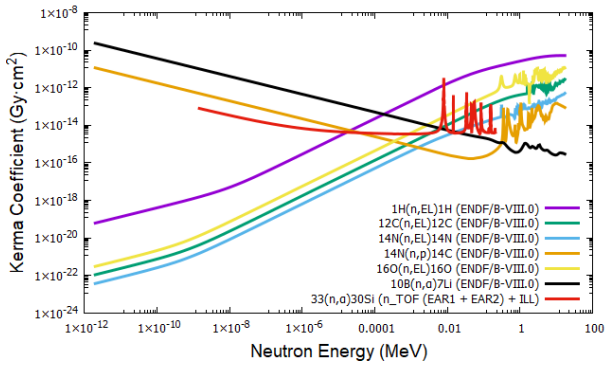

Figure 2. Kerma coefficients of ICRU-4 tissue for neutrons (violet, green, light blue, orange and yellow lines), ^{10}B (ENDF/B-VIII.0) data (black line), ^{33}S (this work data) (red line).

Kerma coefficients for photondepend on the tissue absorption coefficient. They are calculated using the equation (3):

$$k_{f\gamma} = E_\gamma \frac{\mu_{en}}{\rho} \tag{3}$$

where E_γ is the photon energy and $\frac{\mu_{en}}{\rho}$, the absorption coefficient of the selected tissue, taken from NIST [30].

MCNPX code [31] lets simulate the transport and interaction of neutrons with tissue, generating the absorbed dose. For this, it is necessary a file detailing the geometry; in this case, two cylinders, one larger, representing the head, and another one at a depth of 1 cm, which is the tumor; the materials that fill the geometry are also specified to the program, ICRU-4 for the head, and for the tumor, ICRU-4 doped with ^{10}B [7, 28] and ^{33}S [9],

Lee & Zhou [32] showed that for 1920 keV protons impacting on a thick lithium target, neutrons emitted from 70° – 74° to the proton beam have energies ranging from 0 to 20 keV. The highest probability of obtaining 13.5 keV is at 70°. In order to estimate the possible use of ^{33}S as target, it has been considered the case of a pure 13.45 keV homogeneous disk neutron beam of 1 cm radius impacting on the tissue located at 70° of the same section. The tissue contains the proportions of ^{10}B reported in NCT, 40 μg/g [7], and in the case of ^{33}S, the reported for absorption of ^{35}S in mice, 10 mg/g [9]. The considered neutron flux was 10^{10} cm^{-2}·s^{-1} as reported in [28] and the dose rate is considered equal to the kerma rate with the approximation that the energy transferred is equal to the energy absorbed, as usual in this field [7, 28]. Figure 3 shows the result of the dose rate as a function of the depth in tissue.

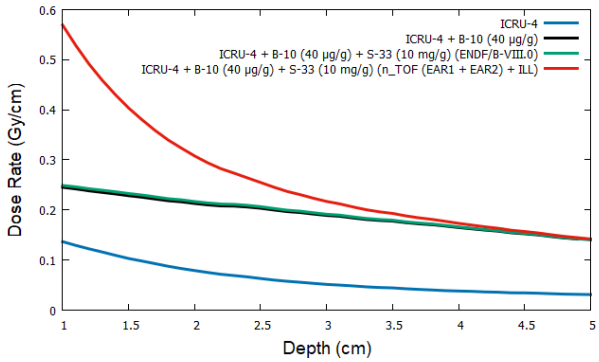

Figure 3. Dose rate due to the incidence of neutrons on: ICRU-4 (blue line); ICRU-4 with ^{10}B (black line); ICRU-4 with ^{10}B and ^{33}S (ENDF/B-VIII.0) (green line); ICRU-4 with ^{10}B and ^{33}S (n_TOF (EAR1 + EAR2) + ILL) (red line); The statistical error is 1.8% for ICRU-4; 0.6% for ICRU-4 with ^{10}B; 1.9% for ICRU-4 with ^{10}B and ^{33}S (ENDF/B-VIII.0); and 2.0% for ICRU-4 with ^{10}B and ^{33}S (n_TOF (EAR1 + EAR2) + ILL).

So, the increment in the dose due to the presence of ^{33}S in the tissue is imperceptibly bigger when the ENDF data are used. However, when the ^{33}S data of the present work are used the dose increases considerably. This sets a good basis for continuing the research on ^{33}S as a cooperative target for NCT.

4 Conclusions

This work reviews the lastest data for the $^{33}S(n,\alpha)^{30}Si$ cross-section. Three experiments were carried out with different objectives. The first one was performed at the EAR1 of n_TOF-CERN facility and provided a value for the Γ_α parameter of the 13.45 keV resonance, which is the most important one, close to the transmission measure of Coddens *et al.* and a factor 1.5 the value obtained in the

(n,α) measurement of Wagemans *et al.* This resonance is crucial to the possible use of ^{33}S in NCT. The second experiment was performed at the EAR2 of the n_TOF-CERN facility and provided for the first time the cross-section from thermal to 10 keV. Furthermore, the area of the 13.45 keV resonance agreed with the value obtained at EAR1, both a factor 1.5 the value of Wagemans *et al.* The third experiment was performed at the PF1B line at ILL nuclear reactor. The aim of the experiment, whose final analysis is ongoing, is to provide a normalization factor to the EAR2 data. The value of the cross-section below 10 keV to thermal is crucial to NCT because the moderation of the neutrons throughout the tissue determines the dose rate delivered to the tumor in depth.

This study proposes the combined use of ^{10}B and ^{33}S as targets for the neutrons in NCT, where the novelty comes from the ^{33}S which has not been used as a target in clinical trials to date and new data used in dose rate simulations. The simulations consider a setup based on the reported data for the absorption of ^{10}B and ^{33}S and neutron yield. A simplification has been performed by considering a monoenergetic neutron beam of 13.45 keV. The results show that the ^{33}S is a promising possibility for NCT.

Acknowlegments. This work has been supported by the Spanish projects FIS2015-69941-C2-1-P (MINECO-FEDER, EU), A-FQM-371-UGR18 (FEDER Andalucia 2014-2020), Spanish Association Against Cancer (AECC) (Grant PS16163811PORR), and the sponsors of the University of Granada Chair Neutrons for Medicine: Fundación ACS, Capitán Antonio and La Kuadrilla.

References

[1] G. F. Auchampaugh *et al.*, Phys. Rev. C **12**, (1975) 1126–33.
[2] C. Wagemans *et al.*, Nucl. Phys. A **469**, (1987) 497-506.
[3] R. Reifarth, K. Schwarz and F. Käppeler. Astrophys. J. **528** (2000) 573-81.
[4] I. Porras. Physics in Medicine and Biology, 2008, 7, 53(7), **L1-9**
[5] NUPECC. Report Nuclear Physics for Medicine, (2014).
[6] National Nuclear Data Center (NNDC) https://www.nndc.bnl.gov/qcalc/.
[7] R. F. Barth, J. A. Coderre *et al.*, Clinical Cancer Research 2005 Jun 1;11(11):3987-4002.
[8] IAEA TECDOC, 2001, Current status of neutron capture therapy. TECDOC-1223.
[9] R. G. Fairchild *et al.*, Cancer Research 1982; 42:5126-5132.
[10] R.S. Kennedy *et al.*, Anticancer Research 15: 2643-9 (2019).
[11] E. J. Seppi. Thesis dissertation 1956. http://www.nndc.bnl.gov/EXFOR/11422.001
[12] F. Münnich, Jour: Zeitschrift für Physik **153**, (1958) 106-123.
[13] J. Benisz, A. Jasielska, and T. Panek. Jour: Acta Physica Polonica, **28** (1965) 763. http://www.nndc.bnl.gov/EXFOR/31032.001.
[14] M. Asghar and A. Emsallem. Conf: 3 Symp. Neutr. Capt. Gamma Ray Spectr. Brookhaven (1978) 549. http://www.nndc.bnl.gov/EXFOR/21302.001.
[15] G. P. Coddens *et al.*, Nucl. Phys. A **469**, (1987) 480-496.
[16] A. J. Kreiner *et al.* Rep Pract Oncol Radiother. 21, 95-101 (2016).
[17] P. Torres-Sánchez, I. Porras *et al.*, Rad. Phys. and Chem. 156 (2019) 240-244.
[18] F. Faghihi and S. Khalili. Rad.. Phys. and Chem. 51 (4–6), 561–569 (2013).
[19] J. Praena *et al.*, Micromegas detector for $^{33}S(n,\alpha)$ cross section measurement at n_TOF. CERN-INT-2012-006 INTC-P-322.
[20] J. Praena *et al.*, $^{33}S(n,\alpha)^{30}Si$ cross section measurement at n_TOF EAR2. CERN-INTC-2015-038 INTC-P-442.
[21] J. Praena *et al.* Research Proposal 67849, ILL Grenoble (2014).
[22] H. Nakamura, ENDF/B-VIII.0:$^{33}S(n,\alpha)^{30}Si$. Evaluated Nuclear Data File (ENDF). https://www-nds.iaea.org/exfor/endf.htm
[23] M. Barbagallo *et al.*, the n_TOF Collaboration. Eur. Phys. J. A (2013) **49**: 156.
[24] J. Praena, M. Sabaté-Gilarte *et al.*, the n_TOF Collaboration, Physical Review, C 97 064603 (2018).
[25] M. Sabaté-Gilarte, M. Barbagallo *et al.*, the n_TOF Collaboration, Eur. Phys. J. A 53 (2017) 210.
[26] M. Sabaté-Gilarte, J. Praena *et al.*, Radiation Protection Dosimetry (2018), vol. 180, No. 1-4, pp. 342-345.
[27] H. Abele *et al.*, Nucl. Instr. and Meth. A 562 407 (2006).
[28] J. T. Goorley *et al.*, Medical Physics, 29(2), 145-156 (2002).
[29] ICRU Report, 1992, Report 46. International Comission on Radiation Units and Measurements, Bethesda, MD.
[30] National Institute of Standards and Technology (NIST) https://physics.nist.gov.html
[31] MCNPX code, Pelowitz, D.B., 2005. MCNPX USER'S MANUAL Version 2.5.0 - LA-CP05-0369, Los Alamos National Laboratory LACP, 2005.
[32] C. L. Lee and X. L. Zhou. Nuclear Instruments and Methods in Physics Research, **B152** (1999) 1-11.